

# Comparison of Threshold-Voltage Shifts for Uniaxial and Biaxial Tensile-Stressed n-MOSFETs

Ji-Song Lim, Scott E. Thompson, *Member, IEEE*, and Jerry G. Fossum, *Fellow, IEEE*

**Abstract**—Large differences in the experimentally observed strain-induced threshold-voltage shifts for uniaxial and biaxial tensile-stressed silicon (Si) n-channel MOSFETs are explained and quantified. Using the deformation potential theory, key quantities that affect threshold-voltage (electron affinity, bandgap, and valence band density of states) are expressed as a function of strain. The calculated threshold-voltage shift is in agreement with uniaxial wafer bending and published biaxial strained-Si on relaxed-Si<sub>1-x</sub>Ge<sub>x</sub> experimental data [1], [2] and explains the technologically important observation of a significantly larger (>4 $\times$ ) threshold-voltage shift for biaxial relative to uniaxial stressed MOSFETs. The large threshold shift for biaxial stress is shown to result from the stress-induced change in the Si channel electron affinity and bandgap. The small threshold-voltage shift for uniaxial process tensile stress is shown to result from the n<sup>+</sup> poly-Si gate in addition to the Si channel being strained and significantly less bandgap narrowing.

**Index Terms**—Biaxial stress, MOSFET, strained silicon, threshold-voltage shift, uniaxial strain.

## I. INTRODUCTION

STRAINED-SILICON MOSFETs (Fig. 1) have been extensively investigated for performance improvements [3]–[9]. Typically, biaxial tensile stress is introduced via a thin epitaxial Si channel grown on a relaxed Si<sub>1-x</sub>Ge<sub>x</sub> substrate. Alternatively, electron mobility enhancement can be obtained using longitudinal uniaxial tensile stress typically introduced with a nitride capping layer [5], [10], [11]. Since the strain capping layer approach requires negligible alterations to a standard CMOS process flow, uniaxial strain is being widely adopted at the 90-nm generation [5], [8], and [11].

Biaxial and uniaxial tensile stress-enhanced electron mobility has been well studied, and shown to result from lower conductivity effective mass in the preferentially occupied  $\Delta_2$  valleys and reduced intervalley scattering [12]. Less attention has been paid to the strain-induced threshold-voltage shifts [13]. The experimental data [1], [2] suggest large threshold-voltage shifts occur for biaxial stress, and much smaller shifts under uniaxial stress [9]. In this letter, we quantitatively explain the experimental results and show that the larger and undesirable threshold-voltage shift for biaxial stress is fundamental to this technique.

Understanding the magnitude of the threshold-voltage shift is important when determining the performance gain of

Manuscript received August 6, 2004. This work was supported by an Applied Materials Graduate Fellowship. The review of this letter was arranged by Editor B. Yu.

The authors are with the Department of Electrical and Computer Engineering, University of Florida, Gainesville, FL 32611-6130 USA (e-mail: jslim@ufl.edu; thompson@ece.ufl.edu).

Digital Object Identifier 10.1109/LED.2004.837581

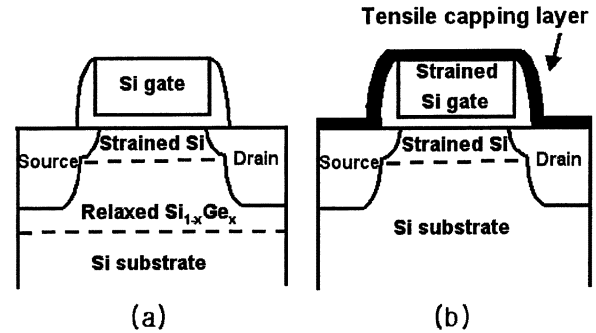


Fig. 1. (a) Biaxial and (b) uniaxial tensile-stressed MOSFET.

strained-Si. Since performance benchmarking needs to be done at constant off-state leakage, an adjustment to compensate for the strain-induced threshold-voltage shift is required. This adjustment is typically accomplished by increasing the well doping concentration which degrades mobility and increases junction capacitance. Recent compact modeling shows half the performance gain is lost when correcting for the large biaxial stress-induced threshold-voltage shift [14].

## II. STRAIN-INDUCED THRESHOLD-VOLTAGE SHIFT

The threshold-voltage expression for biaxial tensile-stressed Si on relaxed Si<sub>1-x</sub>Ge<sub>x</sub> MOSFETs has recently been derived [13]. The same derivation can be used for uniaxial process stress, except strain-induced changes in the n<sup>+</sup> poly-Si gate electron affinity and bandgap need to be included. Unlike wafer substrate strain techniques, an interesting feature of process strain, such as a tensile nitride capping-layer or SiGe in the source and drain [10], is that the Si channel and gate are both strained as shown in Fig. 1. With the gate strain, the expression for the strain-induced threshold-voltage shifts is shown in (1) and (2)

$$q\Delta V_{th}(\sigma) = \begin{cases} (m-1) \left[ \Delta E_g(\sigma) + kT \ln \frac{N_V(0)}{N_V(\sigma)} \right] & \text{for uniaxial tensile stress} \\ \Delta E_C(\sigma) + (m-1) \left[ \Delta E_g(\sigma) + kT \ln \frac{N_V(0)}{N_V(\sigma)} \right] & \text{for biaxial tensile stress} \end{cases} \quad (1) \quad (2)$$

where the last expression (2) is taken from [13],  $\Delta E_C$ ,  $\Delta E_V$ ,  $\Delta E_g$  are the changes in the silicon conduction band, valence band, and energy gap, respectively, and  $m$  is the body-effect coefficient, typically  $\sim 1.3$ – $1.4$ . The terms in (1) and (2) are expressed as a function of stress  $\sigma$  and defined as, for example,  $\Delta V_{th}(\sigma) = V_{th}(\sigma) - V_{th}(0)$ , which denotes the threshold-voltage change before and after stress. Note that  $\Delta E_g(\sigma)$  and  $\Delta E_C(\sigma)$  are negative values, and  $\Delta E_V(\sigma)$  is

positive. In (2), the threshold-voltage shift results from three effects: change in the silicon electron affinity, bandgap, and valence band density-of-states. Also note that (2) for biaxial stress has an additional term  $\Delta E_C(\sigma)$ , compared to (1) for uniaxial stress. This difference results for uniaxial process stress since the electron affinity change for the  $n^+$  poly-Si gate and silicon channel is the same.

### III. CALCULATED RESULTS AND DISCUSSION

In this section, deformation potential theory is used to express  $\Delta E_C$  and  $\Delta E_g$  as a function of strain, which is needed to evaluate (2). The hydrostatic shift and shear splitting of the valence and conduction band edges [15] can be calculated from three classic papers [16]–[18]. In this letter, we calculate the threshold-voltage shift for biaxial and uniaxial tensile-stressed n-channel MOSFETs with  $\langle 110 \rangle$  channel direction on (001) wafers. For these stresses, the conduction band minimum occurs at the two out-of-plane valleys on the  $k_z$  axis ( $\Delta_2$ ). The valence band minimum occurs at the light-hole band for biaxial tensile stress and the heavy-hole band for uniaxial tensile stress. From [16]–[18], we obtain the following expressions for the band-edge shifts due to strain, shown in (3) and (4):

$$\Delta E_C^{(i)}(\sigma) = \Xi_d(\varepsilon_1 + \varepsilon_2 + \varepsilon_3) + \Xi_u \varepsilon_i \quad (3)$$

$$\Delta E_V(\sigma) = \begin{cases} a(\varepsilon_1 + \varepsilon_2 + \varepsilon_3) \pm [b^2(\varepsilon_2 - \varepsilon_3)^2 + (d^2/4)\varepsilon_6^2]^{1/2} \\ \text{for uniaxial } [110] \text{ stress} \\ a(\varepsilon_1 + \varepsilon_2 + \varepsilon_3) + (1/2)(1 \pm 3)(\varepsilon_3 - \varepsilon_1) \\ \text{for biaxial stress} \end{cases} \quad (4)$$

The strain tensor components  $\varepsilon_i$ s linearly depend on stress  $\sigma$  as given by  $\varepsilon_1 = \varepsilon_2 = (S_{11} + S_{12})\sigma/2$ ,  $\varepsilon_3 = S_{12}\sigma$ ,  $\varepsilon_6 = S_{44}\sigma/2$ ,  $\varepsilon_4 = \varepsilon_5 = 0$  for uniaxial  $\langle 110 \rangle$  stress, and  $\varepsilon_1 = \varepsilon_2 = (S_{11} + S_{12})\sigma$ ,  $\varepsilon_3 = 2S_{12}\sigma$ ,  $\varepsilon_4 = \varepsilon_5 = \varepsilon_6 = 0$  for biaxial in-plane stress.

As seen from (3) and (4), the band edge shift results from a hydrostatic term (energy level shift without change in degeneracy) and shear terms, which split the valence and conduction band states ( $\Xi_u, b, d$ ). The shear terms modulate conductivity and mobility. The hydrostatic deformation potential affects important electronic properties such as band gap and electron affinity. The shear deformation potentials are well known with good accuracy from piezoresistance measurements ( $\Xi_u = 9.16$ ,  $b = -2.35$ , and  $d = 5.0$ ) [3], while the hydrostatic deformation can not be directly measured and a very wide range of values (1.13 to  $-10.7$ ) has been reported [4]. Some optical experimental techniques can directly measure differences in the conduction- and valence-band deformation potential, which helps to determine the strain-induced band gap narrowing but still leaves large uncertainty in the electron affinity of strained-Si. Recently, numerical calculations by Fischetti [19] have been used to resolve some of the uncertainty with the hydrostatic deformation potential.

Using Fischetti's recommended deformation potentials (listed in Table I) and (3) and (4), we calculate  $\Delta E_C$  and  $\Delta E_g$  as functions of strain, as listed in Table I. With  $\Delta E_C$  and  $\Delta E_g$ , Fig. 2(a) plots the contribution to the threshold-voltage shift due to the electron affinity and bandgap narrowing terms in (1) and (2). The electron affinity term is the largest factor for

TABLE I  
BAND EDGE DEFORMATION POTENTIAL CONSTANTS,  $\Delta E_C$ , AND  $\Delta E_g$   
CALCULATED VERSUS STRAIN (YOUNG'S MODULI,  $E_{[110]} \cong 169$   
GPa AND  $E_{[100]} \cong 130$  GPa USED)

Stress type	Deformation potential constants [eV]	$\Delta E_C(\sigma)$ [eV]	$\Delta E_g(\sigma)$ [eV]
[110] Uniaxial	$\Xi_d = 1.13$ $\Xi_u = 9.16$	$a = 2.46$ $b = -2.35$ $d = -5.08$	$-2.66\varepsilon$ $-6.19\varepsilon$
Biaxial (1)	$\Xi_d = 1.13$ $\Xi_u = 9.16$	$a = 2.46$ $b = -2.35$	$-5.67\varepsilon$ $-17.01\varepsilon$
Biaxial (2)	$\Xi_d = -10.7$ $\Xi_u = 10.5$	$a = -9.7$ $b = -2.33$	$-41.04\varepsilon$ $-44.72\varepsilon$

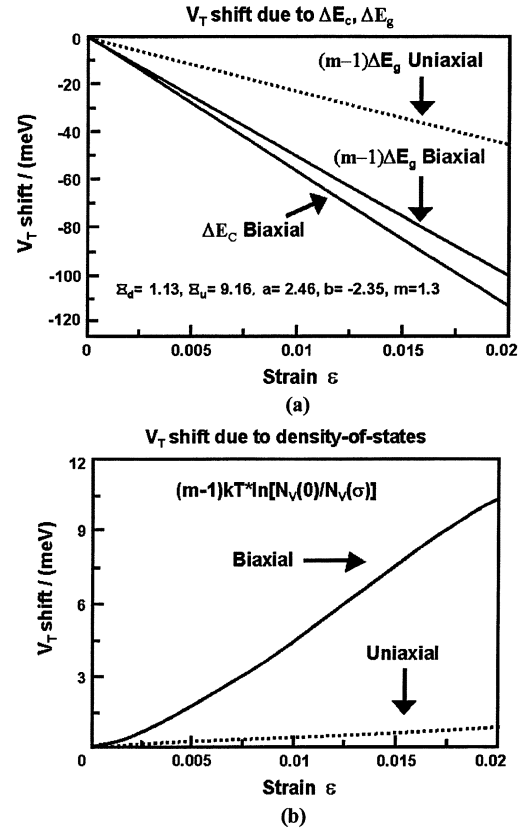


Fig. 2. Plot of key parameters in  $\Delta V_{th}(\sigma)$ : (a)  $\{\Delta E_C(\sigma)$  and  $(m - 1)\Delta E_g(\sigma)\}$  and (b)  $kT \ln[N_V(0)/N_V(\sigma)]$  versus strain.

biaxial stress, but bandgap narrowing is also a significant factor. Fig. 2(a) also shows the bandgap narrowing term is larger for biaxial stress than uniaxial stress, which will be discussed in the next paragraph. Lastly, to bracket the uncertainty in the threshold-voltage shift, a second set of deformation potentials [19] is given in Table I, which will be discussed at the end.

In addition to electron-affinity and bandgap-narrowing terms, stress-induced changes in the density-of-states also shift the threshold-voltage (last term in (1) and (2)). For uniaxial and biaxial tensile stress, the heavy- and light-hole bands are shifted up in energy, respectively. From (4), this creates larger bandgap narrowing for biaxial stress since a larger shift occurs for the light- than heavy-hole band. The density-of-states in the valence-band is defined as  $N_V \equiv 2[2\pi kT m_p^*/\hbar^2]^{3/2}$

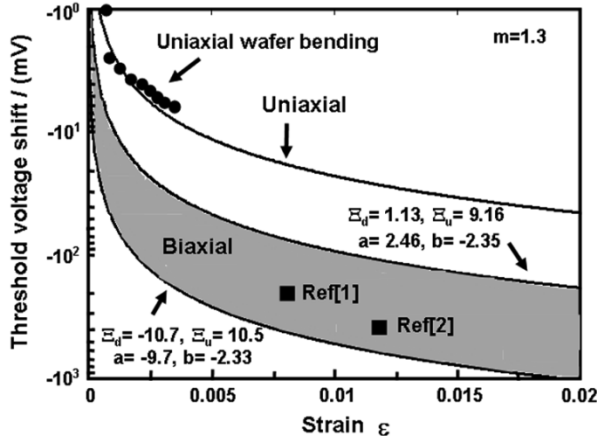


Fig. 3. Biaxial and uniaxial stressed Si MOSFET threshold-voltage shifts versus strain.

where the hole effective mass  $m_p \equiv [m_{lh}^{3/2} + m_{hh}^{3/2}]^{2/3}$ , and  $m_{lh}$  and  $m_{hh}$  are the light- and heavy-hole masses, respectively. Thus, the change in density-of-states is given by  $N_V(0)/N_V(\sigma) = m_p^*(0)^{3/2}/m_p^*(\sigma)^{3/2}$ . The expressions for the hole effective mass  $m_p^*(\sigma)$  are obtained as shown in (5)

$$m_p^*(\sigma) = \begin{cases} \left[ m_{lh}^{3/2} * H(\sigma)^{3/2} + m_{hh}^{3/2} \right]^{2/3} & \text{for uniaxial [110] tensile stress} \\ \left[ m_{lh}^{3/2} + m_{hh}^{3/2} * H(\sigma)^{3/2} \right]^{2/3} & \text{for biaxial in-plane tensile stress} \end{cases} \quad (5)$$

where

$$H(\sigma) \equiv \exp \left[ -\frac{|\Delta E_{lh}(\sigma)| + |\Delta E_{hh}(\sigma)|}{kT} \right].$$

Fig. 2(b) plots the threshold-voltage shifts due to the change in valence-band density-of-states. Again for biaxial stress, the density-of-states term contributes more, but in general the density-of-states contribution to the threshold-voltage shift is small compared to the electron-affinity and bandgap-narrowing terms.

Finally, we note that the above formalism for  $\Delta E_c$  and  $\Delta E_g$  is identical to the classic paper by Peoples [21], which resulted in the classic and commonly used expression for biaxial tensile-strained-Si bandgap narrowing of  $\Delta E_g = 0.4x$  eV, where  $x$  is the Ge concentration in the SiGe substrate. However, using the most recently accepted deformation potentials results in  $\Delta E_g = 0.68x$  eV. To bracket the uncertainty in the electron affinity, the entire range of the dilation deformation (1.1.3 to  $-10.7$ ) is used. Fig. 3 plots the threshold-voltage shift for uniaxial and biaxial stress with the two sets of deformation potentials. Also included in Fig. 3 is experimental data for n-MOSFET threshold-voltage shift due to uniaxial tensile stress, obtained using a four-point bending method, and reported literature values for biaxial stress obtained with  $\text{Si}_{1-x}\text{Ge}_x$  substrates. The experimental data agree well with the calculated results. Using the range of dilation deformation potentials, the calculated biaxial stress-induced threshold-voltage

shift brackets the experimental data and supports the conclusion that the shift is at least  $4\times$  larger than for uniaxial stress.

#### IV. CONCLUSION

In summary, the large difference in the experimentally observed threshold-voltage shifts for uniaxial and biaxial stressed silicon n-channel MOSFETs are explained and quantified. The small threshold-voltage shift for uniaxial process strain is shown to result from less band gap narrowing and the  $n^+$  poly gate being strained.

#### REFERENCES

- [1] Q. Xiang, J.-S. Goo, J. Pan, B. Yu, S. Ahmed, J. Zhang, and M.-R. Lin, "Strained silicon NMOS with nickel-silicide metal gate," in *Symp. VLSI Tech. Dig.*, 2003, pp. 101–102.
- [2] N. Sugii *et al.*, "Performance enhancement of strained-Si MOSFETs fabricated on a chemical-mechanical-polished SiGe substrate," *IEEE Trans. Electron Devices*, vol. 49, pp. 2237–2243, Dec. 2002.
- [3] H. Miyata, T. Yamada, and D. K. Ferry, "Electron transport properties of a strained-Si layer on a relaxed  $\text{Si}_{1-x}\text{Ge}_x$  substrate by Monte Carlo simulation," *Appl. Phys. Lett.*, vol. 62, pp. 2661–2663, 1993.
- [4] K. Rim, J. Welsler, J. L. Hoyt, and J. F. Gibbons, "Enhanced hole mobilities in surface-channel strained-Si p-MOSFETs," in *IEDM Tech. Dig.*, 1995, pp. 517–520.
- [5] S. Thompson *et al.*, "A 90 nm logic technology featuring 50 nm strained silicon channel transistors, 7 layers of Cu interconnects, low k ILD, and 1 mm<sup>2</sup> SRAM cell," in *IEDM Tech. Dig.*, 2002, pp. 61–64.
- [6] J. Goo *et al.*, "Scalability of strained-Si n-MOSFETs down to 25 nm gate length," *IEEE Electron Device Lett.*, vol. 24, pp. 351–353, Apr. 2003.
- [7] K. Rim *et al.*, "Characteristics and device design of sub-100 nm strained-Si N- and PMOSFETs," in *Symp. VLSI Tech. Dig.*, 2002, pp. 98–99.
- [8] V. Chan *et al.*, "High speed 45 nm gate length CMOSFETs integrated into a 90 nm bulk technology incorporating strain engineering," in *IEDM Tech. Dig.*, 2003, pp. 77–80.
- [9] W. Zhao, J. He, R. E. Belford, L. E. Wernersson, and A. Seabaugh, "Partially depleted SOI MOSFETs under uniaxial tensile strain," *IEEE Trans. Electron Devices*, vol. 51, pp. 317–323, Feb. 2003.
- [10] S. E. Thompson *et al.*, "A logic nanotechnology featuring strained silicon," *IEEE Electron Device Lett.*, vol. 25, pp. 191–193, Apr. 2004.
- [11] K. Rim, K. Chan, L. Shi, D. Boyd, J. Ott, N. Klymko, F. Cardone, L. Tai, S. Koester, M. Cobb, D. Canaperi, B. To, E. Duch, I. Babich, R. Carruthers, P. Saunders, G. Walker, Y. Zhang, M. Steen, and M. Jeong, "Fabrication and mobility characteristics of ultra-thin strained Si directly on insulator (SSDOI) MOSFETs," in *IEDM Tech. Dig.*, 2003, pp. 49–52.
- [12] S. Takagi, J. L. Hoyt, J. J. Welsler, and J. F. Gibbons, "Comparative study of phononlimited mobility of two-dimensional electrons in strained and unstrained-Si metal-oxide-semiconductor field-effect transistors," *J. Appl. Phys.*, vol. 80, pp. 1567–1577, 1996.
- [13] W. Zhang and J. G. Fossum, "On the threshold voltage of strained-Si- $\text{Si}_{1-x}\text{Ge}_x$  MOSFETs," *IEEE Trans. Electron Devices*, submitted for publication.
- [14] J. G. Fossum and W. Zhang, "Performance projections of scaled CMOS devices and circuits with strained-Si-on-SiGe channels," *IEEE Trans. Electron Devices*, vol. 50, pp. 1042–1048, Apr. 2003.
- [15] C. T. Sah, *Fundamentals of Solid-State Electronics*. Singapore: World Scientific, 1995.
- [16] C. Herring and E. Vogt, "Transport and deformation-potential theory for many-valley semiconductors with anisotropic scattering," *Phys. Rev.*, vol. 101, pp. 944–961, 1956.
- [17] I. Balslev, "Influence of uniaxial stress on the indirect absorption edge in silicon and germanium," *Phys. Rev.*, vol. 143, pp. 636–647, 1966.
- [18] C. G. VandeWalle and R. M. Martin, "Theoretical calculations of heterojunction discontinuities in the Si/Ge system," *Phys. Rev. B, Condens. Matter*, vol. 34, pp. 5621–5634, 1986.
- [19] M. V. Fischetti and S. E. Laux, "Band structure, deformation potentials, and carrier mobility in strained-Si, Ge, and SiGe alloys," *J. Appl. Phys.*, vol. 80, pp. 2234–2252, 1996.
- [20] R. People, "Indirect band gap of coherently strained  $\text{Ge}_x\text{Si}_{1-x}$  bulk alloys on (001) silicon substrates," *Phys. Rev. B, Condens. Matter*, vol. 32, pp. 1405–1408, 1985.